Environmental Science & Technology

Article

Cite This: Environ. Sci. Technol. XXXX, XXX, XXX−XXX

pubs.acs.org/est

Enhanced Capabilities of TROPOMI NO_2: Estimating NO_X from North American Cities and Power Plants

Daniel L. Goldberg,*[,†,‡,△] Zifeng Lu,[†,‡] David G. Streets,[†,‡] Benjamin de Foy,[§] Debora Griffin,[∥] Chris A. McLinden,[∥] Lok N. Lamsal,[⊥,#] Nickolay A. Krotkov,[#] and Henk Eskes[¶]

[†]Energy Systems Division, Argonne National Laboratory, Lemont, Illinois 60439, United States

[‡]Consortium for Advanced Science and Engineering, University of Chicago, Chicago, Illinois 60637, United States

[△]Department of Environmental and Occupational Health, George Washington University, Washington, DC 20052, United States

[§]Department of Earth and Atmospheric Sciences, Saint Louis University, St. Louis, Missouri 63108, United States

[∥]Air Quality Research Division, Environment and Climate Change Canada, Toronto, Ontario M3H 5T4, Canada

[⊥]University Space Research Association, Goddard Earth Sciences Technology and Research (GESTAR), Columbia, Maryland 21046, United States

[#]NASA Goddard Space Flight Center, Greenbelt, Maryland 20770, United States

[¶]Royal Netherlands Meteorological Institute (KNMI), De Bilt 3730 AE, The Netherlands

Supporting Information

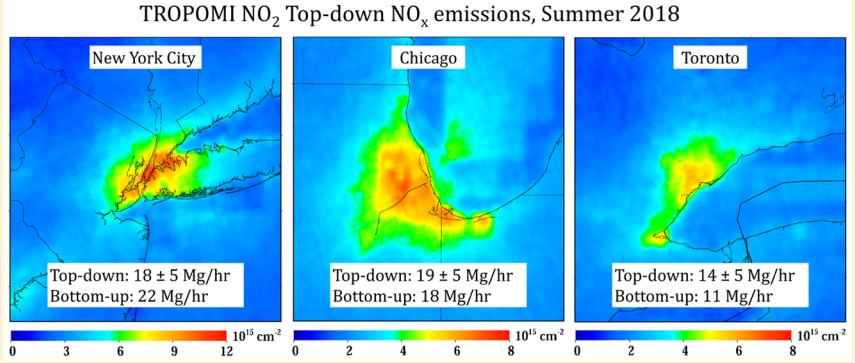

ABSTRACT: The TROPOspheric Monitoring Instrument (TROPOMI) is used to derive top-down NO_X emissions for two large power plants and three megacities in North America. We first re-process the vertical column NO_2 with an improved air mass factor to correct for a known systematic low bias in the operational retrieval near urban centers. For the two power plants, top-down NO_X emissions agree to within 10% of the emissions reported by the power plants. We then derive top-down NO_X emissions rates for New York City, Chicago, and Toronto, and compare them to projected bottom-up emissions inventories. In this analysis of 2018 NO_X emissions, we find a +22% overestimate for New York City, a −21% underestimate in Toronto, and good agreement in Chicago in the projected bottom-up inventories when compared to the top-down emissions. Top-down NO_X emissions also capture intraseasonal variability, such as the weekday versus weekend effect (emissions are +45% larger on weekdays versus weekends in Chicago). Finally, we demonstrate the enhanced capabilities of TROPOMI, which allow us to derive a NO_X emissions rate for Chicago using a single overpass on July 7, 2018. The large signal-to-noise ratio of TROPOMI is well-suited for estimating NO_X emissions from relatively small sources and for sub-seasonal timeframes.

INTRODUCTION

NO_X ($NO_X \equiv NO + NO_2$) is a group of toxic air pollutants primarily created as a byproduct of fossil fuel or biomass combustion. NO_X can participate in a series of chemical reactions to generate O_3 (a toxic air pollutant with a longer atmospheric lifetime), HNO_3 (a key contributor to acid rain), and particulate nitrate (NO_3^-) (a component of fine particulate matter and an additional health hazard).[1] NO_X is unique because of its short photochemical lifetime (2−8 h) during the summer daytime.[2−4] As a result, tropospheric NO_X concentrations are strongly correlated with local emissions, which are often anthropogenic in origin.

There is a rich legacy of monitoring NO_X by remote sensing instruments.[5] NO_2—which approximately comprises 70% of NO_X in urban areas[6]—can be observed from space because it

Received: July 25, 2019
Revised: October 9, 2019
Accepted: October 11, 2019
Published: October 11, 2019

DOI: 10.1021/acs.est.9b04488
Environ. Sci. Technol. XXXX, XXX, XXX−XXX

has unique high frequency spectral features within the 400−500 nm wavelength region.[7] The newest remote sensing spectrometer, TROPOMI,[8,9] has been gathering data on the global heterogeneities of NO_2 air pollution since October 2017. This instrument builds on the legacy of prior ultraviolet−visible (UV−vis) spectrometers including the Global Ozone Monitoring Experiment (GOME),[5,10,11] Scanning Imaging Spectrometer for Atmospheric Chartography (SCIAMACHY),[12,13] Global Ozone Monitoring Experiment-2 (GOME-2),[14,15] and the Ozone Monitoring Instrument (OMI).[16−19]

The short lifetime of NO_2 has been exploited to infer NO_X emissions from satellite remote sensing instruments in various areas around the globe.[2−4,20−27] Because of continuous methodology improvements over the past decade, deriving NO_X emissions from NO_2 satellite observations can be done with high accuracy.[27] However, because of the coarse pixel size of previously launched sensors (varying from 13 × 24 km^2 at nadir by OMI to 40 × 320 km^2 by GOME), these instruments were primarily used to generate emissions estimates over long timeframes (>12 months) by oversampling to finer resolution (e.g., 4 × 4 km^2).[21,24,26] While these long-term emissions estimates are helpful, the magnitude of NO_X emissions changes daily and seasonally—because of fossil fuel demands—and annually—because of regulations and economic drivers. As a result, long-term averages of NO_X emissions are not ideal for policy regulators.

TROPOMI's smallest pixel size (3.5 × 7.2 km^2 at nadir, reduced to 3.5 × 5.6 km^2 at nadir on August 6, 2019) and enhanced signal-to-noise ratio are significant improvements when compared to previous satellite instruments.[8] Initial NO_2 measurements from TROPOMI show the complex spatial heterogeneities of NO_2 pollution far better than any instrument before it.[28] In this paper, we show subseasonal NO_X emissions estimates from three megacities in eastern North America and two isolated power plants in the western United States. We use a method originally developed by Beirle et al.[2] and refined by later studies[3,24,27] to derive monthly NO_X emission estimates using a statistical fit of NO_2 column measurements with an exponentially modified Gaussian (EMG) function. The results shown here represent the first time NO_X emissions have been derived for subseasonal periods.

METHODS

TROPOMI was launched by the European Space Agency (ESA) for the European Union's Copernicus Sentinel 5 Precursor (S5p) satellite mission on October 13, 2017. The satellite follows a sun-synchronous, low-earth (825 km) orbit with an equator overpass time of approximately 13:30 local solar time. TROPOMI measures total column amounts of several trace gases in the UV−vis−near infrared−shortwave infrared spectral regions. At nadir, pixel sizes are 3.5 × 7.2 km^2 with little variation in pixel sizes across the 2600 km swath. The instrument observes the swath approximately once every second and orbits the Earth in about 100 min, resulting in daily global coverage. NO_2 slant column densities are derived from radiance measurements in the 405−465 nm spectral window of the UV−vis−NIR spectrometer.[9] Tropospheric vertical column density data, which represent the vertically integrated number of NO_2 molecules per unit area between the surface and the tropopause, are then calculated by subtracting the stratospheric portion and then converting the tropospheric slant column to a vertical column a posteriori using an air mass factor (AMF). The AMF is a unitless quantity used to convert the slant column into a vertical column and is a function of the satellite viewing angles, solar angles, the effective cloud radiance fraction and pressure, the vertical profile shape of NO_2 provided by a chemical transport model simulation (for operational data TM5-MP model is used at 1° × 1° resolution), and the surface reflectivity (for operational data, OMI climatological Lambertian equivalent reflectivity is used at a 0.5° × 0.5° resolution).[29] The operational AMF calculation does not explicitly account for aerosol absorption effects, which are accounted for in the effective cloud radiance fraction.

For this study, we use the operational TROPOMI NO_2 total slant column (SCD_{total}) and stratospheric slant column (SCD_{strat}) NO_2 products as provided by KNMI, and tropospheric AMF (AMF_{trop}) provided by Environment and Climate Change Canada (ECCC) to calculate tropospheric vertical column amounts (VCD_{trop}) using eq 1.

$$VCD_{trop} = \frac{SCD_{total} - SCD_{strat}}{AMF_{trop}} \quad (1)$$

The ECCC tropospheric vertical column product is derived from the operational v1 (varies from v1.00.01 to v1.01.00) TROPOMI NO_2 data, which have been publicly released starting April 30, 2018. In the ECCC TROPOMI NO_2 tropospheric vertical column product, the tropospheric AMF has been re-processed to include daily mid-afternoon vertical NO_2 shape factors from a 10 × 10 km^2 Global Environmental Multiscale-Modelling Air-quality and Chemistry (GEM-MACH) chemical transport model simulation and MODIS 0.01° × 0.01° surface reflectance. For more details on the AMF methodology, please refer to McLinden et al. and Griffin et al.[28,30] We filter the TROPOMI NO_2 data to ensure only the best quality pixels are used. Daily pixels with solar zenith angles ≥80° and cloud radiance fractions ≥0.5 are removed.

An EMG function (described in detail in the next paragraph) is fit to an oversampling of re-processed NO_2 column measurements observed by TROPOMI around each point source (i.e., power plant or city) rotated based on wind direction in order to determine the NO_2 burden and lifetime within the average plume. The NO_2 plumes for each day were rotated based on the wind direction of the bottom eight levels (i.e., from the surface to ∼500 m) of the 0.125° × 0.125° ERA-Interim re-analysis[31] and then manually adjusted to ensure that the plume was oriented from west to east. Because we discovered that this analysis is very sensitive to the wind direction, we have completed the time-consuming step of manually adjusting every day of the TROPOMI NO_2 record using visual inspection so that each day's NO_2 plume is aligned from west to east. Most days need between 0° and 30° of manual rotation. Therefore, the ERA-Interim wind direction provides a first guess, but any errors associated with the wind direction are minimized by the manual rotation. Only days in which the ERA-Interim wind speeds are >3 m/s are included in this analysis because NO_2 decay under this condition is dominated by chemical removal, not variability in the winds.[4] For the power plants in the western U.S., it was necessary to relax this threshold to >1 m/s because synoptic winds during summer in the western U.S. are often weak.

The original methodology, proposed by Beirle et al.[2] and applied to OMI NO_2 data,[3,23,24,27] involves the fitting of

DOI: 10.1021/acs.est.9b04488
Environ. Sci. Technol. XXXX, XXX, XXX−XXX

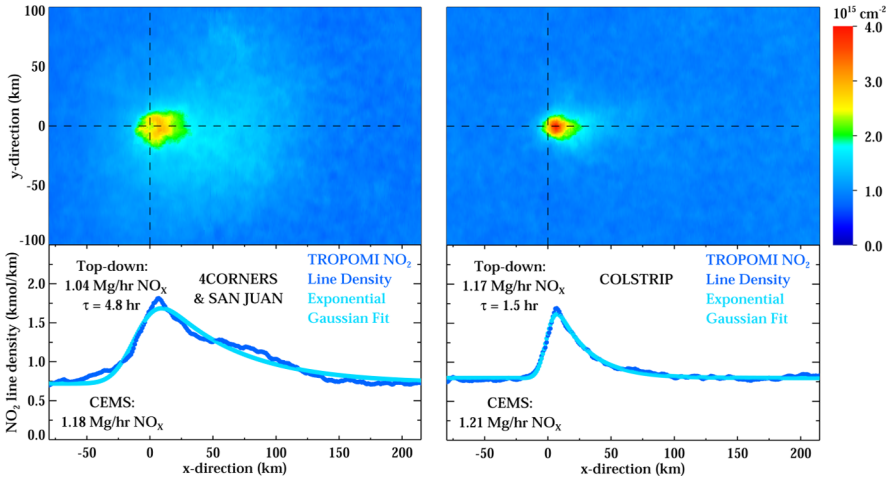

Figure 1. Average May to Sept 2018 top-down NO_X emissions estimates from two isolated power plant complexes in the western U.S.: (left) Four Corners/San Juan, NM and (right) Colstrip, MT. Top panels show the TROPOMI NO_2 data rotated based on wind direction. Only days with 0–500 m averaged wind speeds >1 m/s and 75% valid coverage within a 1° × 1° box centered on the source are used. Bottom panels show the TROPOMI NO_2 line densities, which are integrals along the *y*-axis ± 25 km about the *x*-axis. The statistical EMG fit to the top-down line densities is shown in light blue.

satellite NO_2 line densities to an EMG function. In this manner, the average NO_X emissions rate and effective photochemical lifetime of NO_2 can be derived from the parameters that describe the best statistical fit.

NO_2 line densities are the integral of the NO_2 satellite retrieval perpendicular to the path of the plume; the units are mass per distance. The EMG model is expressed as

$$\text{TROPOMI NO}_2\text{ line density} = \alpha\left[\frac{1}{x_o}\exp\left(\frac{\mu}{x_o}+\frac{\sigma^2}{2x_o^2}-\frac{x}{x_o}\right)\Phi\left(\frac{x-\mu}{\sigma}-\frac{\sigma}{x_o}\right)\right]+\beta \quad (2)$$

where α is the total number of NO_2 molecules observed near the hotspot, excluding the effect of background NO_2, β; x_o is the e-folding distance downwind, representing the length scale of the NO_2 decay; μ is the location of the apparent source relative to the city center; σ is the standard deviation of the Gaussian function, representing the Gaussian smoothing length scale; and Φ is the cumulative distribution function. Using the "curvefit" function in IDL, we determine the five unknown parameters: α, x_o, σ, μ, and β based on the independent (distance; x) and dependent (TROPOMI NO_2 line density) variables.

Using the mean ERA-Interim wind speed, w, of the NO_2 line density domain, the mean effective NO_2 lifetime $\tau_{effective}$ and mean NO_X emissions can be calculated from the fitted parameters x_o and α

$$\text{NO}_X\text{ emissions} = 1.33\left(\frac{\alpha}{\tau_{effective}}\right), \qquad \text{where } \tau_{effective} = \frac{x_o}{w} \quad (3)$$

The factor of 1.33 is the mean column-averaged NO_X/NO_2 ratio and is time-dependent, spatially varying, and primarily a function of the localized $j(NO_2)$ and O_3 concentration.

RESULTS

To validate our top-down NO_X emissions, we test our methodology on known NO_X emissions sources: large U.S. power plants. Air pollutant emissions from large U.S. power plants are tracked hourly by EPA's continuous emission monitoring systems (CEMS) database (https://ampd.epa.gov/ampd/). Pollutant flow rates are measured continuously inside the power plant stacks, and the data are quality-assured using the procedures described by federal guidelines (Appendix F to 40 CFR 60). To ensure that our top-down method is quantifying the emissions of the selected power plant without contamination from other sources, we choose power plants in isolated areas far from any other large source of NO_X emissions. For our analysis, we choose the Four Corners/San Juan Power Plant complex in New Mexico and the Colstrip Power Plant in Montana. These power plant complexes are analyzed because of their persistently detectible NO_X emissions over short timeframes and isolated nature. These power plants have legacies for being some of the largest point-source NO_X emitters in the United States. Other power plants were considered, but their plumes were not consistently detected on daily timeframes; we expect that if this analysis were conducted over a longer timeframe, we would remove the requirement of having a detectable daily plumes and thus would be able to analyze the NO_X emissions of other power plants.

In Figure 1, we show the top-down NO_X emissions derivation for the Four Corners/San Juan and Colstrip power plants. For a five-month period during May to September 2018 (154 days), the top-down NO_X emissions for Four Corners/San Juan are only 12% smaller than reported in the CEMS database. For the same five-month period, the top-down NO_X emissions for Colstrip are 3% smaller than reported in the CEMS database. In each case, the daily CEMS NO_X emissions rates during the early afternoon (11 AM to 2 PM local time) are temporally matched to days with valid TROPOMI overpasses. In total, there are 90 TROPOMI overpasses used for the Four Corners/San Juan top-down derivation and 92 TROPOMI overpasses for Colstrip. When using the operational tropospheric vertical column product provided by KNMI, we find a larger underestimate of 25 and 28% respectively (Figure S1), which indicates that re-processing the AMF with the GEM-MACH regional chemical

DOI: 10.1021/acs.est.9b04488
Environ. Sci. Technol. XXXX, XXX, XXX−XXX

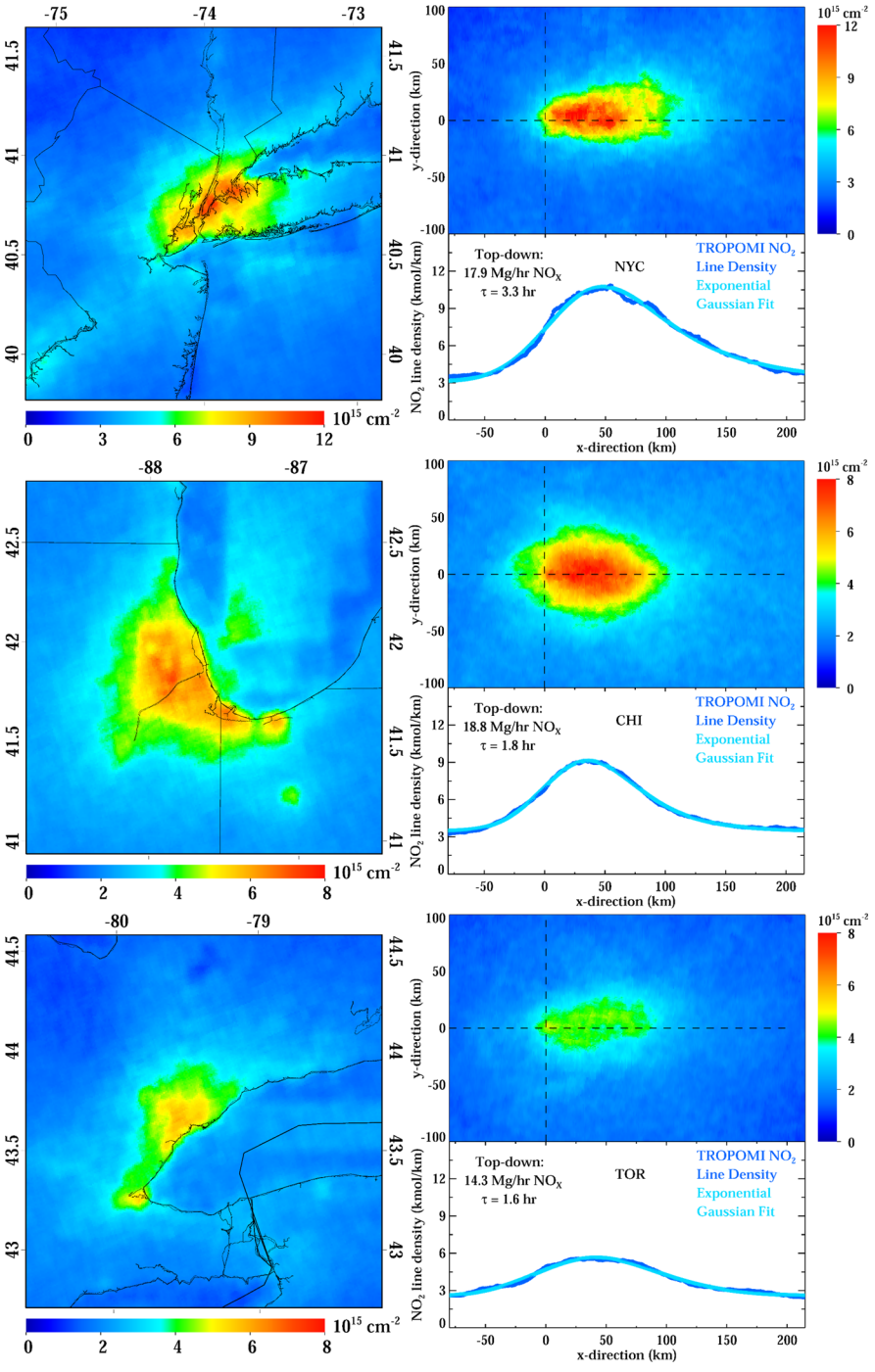

Figure 2. (Left) TROPOMI NO_2 oversampled to 1 km resolution for May−Sept 2018 for the (top) New York City area, (center) Chicago area, and (bottom) Toronto area. (Right) Five-month averaged top-down NO_X emissions estimates from these three cities: top panels show the TROPOMI NO_2 data rotated based on wind direction. Only days with 0−500 m averaged wind speeds >3 m/s and 75% coverage within a 1° × 1° box centered on the source are used, while bottom panels show the TROPOMI NO_2 line densities, which are integrals along the *y*-axis ± 50 km about the *x*-axis. The statistical EMG fit to the top-down line densities is shown in light blue.

transport model is moderating a systematic low bias in the operational retrieval.

This methodology is then applied to three megacities—New York City, Chicago, and Toronto—in North America that have consistent and distinguishable NO_X plumes originating from pollution sources in the city centers. We choose these cities because of their legacies of have large NO_X emissions, flat topography, and propensity for moderate wind speeds during summer. These cities are susceptible to sea and lake breezes, but these are minimized during days with strong synoptic winds (>3 m/s). Other cities were considered, but their plumes were not consistently detected on daily timeframes or their synoptic winds were too weak (e.g., Los Angeles); we expect that if this analysis were conducted over a longer timeframe, we would remove these requirements and thus would be able to analyze the NO_X emissions of additional cities.

DOI: 10.1021/acs.est.9b04488
Environ. Sci. Technol. XXXX, XXX, XXX−XXX

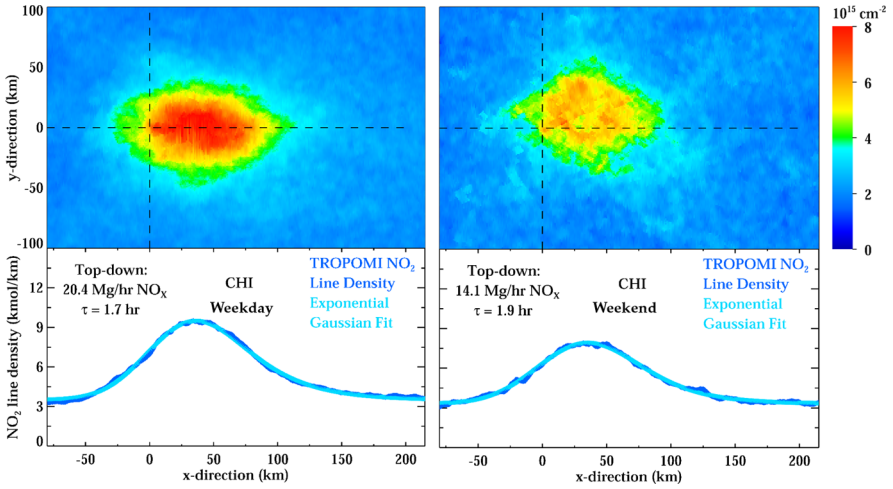

Figure 3. Five-month averaged top-down NO_X emissions estimates for Chicago sorted by weekdays and weekends during the summer of 2018. (Left) Weekdays only (28 days total) and (right) weekend days only (10 days total).

For our analysis of city emissions rates, we only use TROPOMI NO_2 overpass data that fit three criteria: 0−500 m re-analysis wind speeds are >3 m/s, >75% of the area within a 50 km radius of the city center has a valid TROPOMI NO_2 retrieval, and there is an identifiable plume originating from the city that is larger than any other plume within 100 km upwind or downwind of the city. The latter criterion is done by visual inspection and is used to eliminate contamination from other cities in the region, such as the effects of Philadelphia on New York during days with southwesterly synoptic winds or the effects of Milwaukee on Chicago on days with northerly synoptic winds. During these mostly clear and completely clear days, any given grid point has an 87% chance of having a valid pixel. In other words, on these mostly clear days, there is a very high chance that almost all of the metropolitan area has a valid retrieval.

In Figure 2, we show the top-down method applied to these three cities for the five-month period of May to September 2018. For New York City, the five-month top-down estimate is 18 Mg/h NO_X. The five-month timeframe (154 days total) only elicited 24 valid days—20 weekdays and 4 weekend days; this five-month period was the wetter and cloudier than normal for New York City.[32] The 18 Mg/h estimate is lower than the projected 2018 EPA NEI NO_X emissions rate of 22 Mg/h within a 50 km radius of the city; the projected 2018 value is calculated by assuming a 5% per year reduction in NO_X since the 2014 NEI. The discrepancy between the bottom-up inventory and the top-down approach can be attributed to three compounding factors: a potential small systematic low bias in the retrieval, the bottom-up NO_X from the 2014 NEI may be too large, or the 5% per year reduction is too conservative. It should be noted, however, that an overestimate in the NEI is consistent with other studies in the mid-Atlantic.[33,34] For Chicago, the five-month top-down estimate is 19 Mg/h NO_X. The five-month timeframe elicited 38 valid days—28 weekdays and 10 weekend days. For Chicago, we find excellent agreement with projected 2018 NEI annual average of 18 Mg/h. For Toronto, the five-month top-down estimate is 14 Mg/h NO_X over 39 days—30 weekdays and 9 weekend days. Projected emissions inventories within a 50 km radius of Toronto (excluding nearby Hamilton) are 11 Mg/h;[35] thus, there appears to be an underestimate in NO_X emissions for Toronto. When using the operational tropospheric vertical column product, top-down emissions are 36−47% smaller than the top-down emissions described above (Figure S2).

In order to quantify the uncertainty associated with the top-down NO_X estimates, we use a bootstrapping technique to evaluate the sensitivity of the estimates to the selection of days.[4] In this method, we randomly replace entire daily TROPOMI scenes with scenes from other days. We perform this random replacement 100 times to generate a distribution of estimates around the mean top-down NO_X estimates. For New York City, the NO_X bootstrapped emissions are 18 ± 5 Mg/h, yielding a coefficient of variation (standard deviation/mean) of 0.26. For Chicago, the NO_X bootstrapped emissions are 19 ± 5 Mg/h, yielding a coefficient of variation of 0.27. For Toronto, the NO_X bootstrapped emissions are 14 ± 5 Mg/h, yielding a coefficient of variation of 0.36. This suggests that the top-down NO_x emissions have an uncertainty of about 30% because of daily variability; it should be noted that bootstrapping does not account for any systematic bias in the measurements, such as those related to a clear-sky bias (e.g., emissions patterns may be different on cloudier and cooler days).[36]

We then calculate the NO_X emissions over shorter timescales in order to assess the sub-seasonal variability of NO_X emissions. We separate the satellite data into weekday and weekend bins. In Figure 3, we find the NO_X emission rate to be 45% larger on weekdays when compared to weekend days in Chicago. Similar findings have been documented elsewhere,[37,38] but this is the first time it has been documented using a single season of satellite data.

In a final step, we discovered a day in which NO_X emissions could be derived using a single TROPOMI overpass. On July 7, 2018—a Saturday—a plume originating from the Chicago metropolitan area can be clearly observed. The following unique combination of factors allowed us to derive top-down NO_X emissions using a single overpass: there were no clouds within a 200 km radius of the city, the wind speed was strong enough (>3 m/s) to observe a decaying downwind plume, and the unique wind direction (ESE) was such that there was no contamination from upwind or downwind sources. For this day, we derived the top-down NO_X emissions rate to be 11.5 Mg/h, as seen in Figure 4. This estimate is similar to the five-month weekend emissions rate, which gives us confidence that

DOI: 10.1021/acs.est.9b04488
Environ. Sci. Technol. XXXX, XXX, XXX−XXX

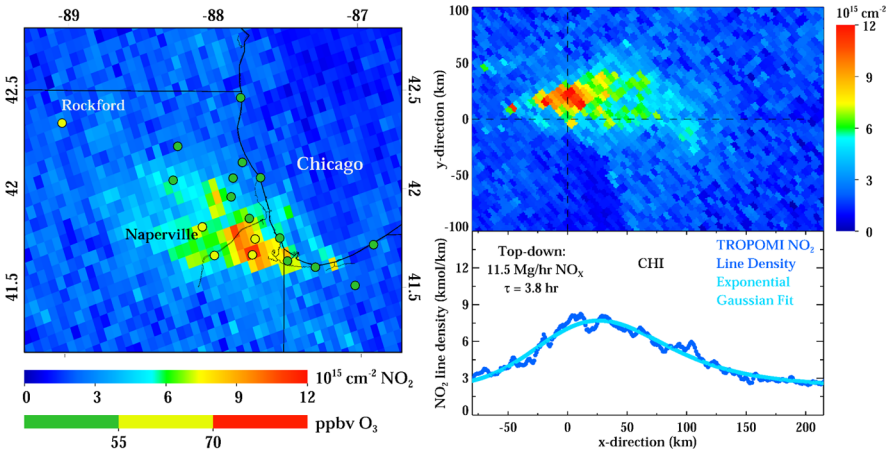

Figure 4. Daily top-down NO_X emissions estimate for the Chicago area on Saturday July 7, 2018. (Left) Observed operational TROPOMI NO_2 columns and 8 h maximum ozone concentrations from the EPA AQS shown as colored circles. (Right) Top panel shows the TROPOMI NO_2 re-processed data rotated based on the daily wind direction (ESE). The bottom panel shows the re-processed TROPOMI NO_2 line densities, which are integrals along the *y*-axis ± 50 km about the *x*-axis. The statistical EMG fit to the top-down line densities is shown in light blue.

this estimate is robust. In Figure 4, we also provide surface 8 h maximum O_3 measurements at EPA air quality system (AQS) monitoring stations on that day. At the beginning of the plume—the Illinois/Indiana border—there are no enhancements of O_3. However, as the observed plume progresses downwind, there are 15−20 ppb enhancements of surface O_3. At the Naperville, IL EPA AQS monitor, observed 8 h maximum daily O_3 reached 58 ppb and at the Rockford, IL AQS monitor, 8 h maximum daily O_3 reached 62 ppb. This suggests that O_3 production is NO_X-limited within the majority of the downwind plume. This also suggests that the Chicago metropolitan area was responsible for the enhancements of O_3 in the western suburbs on this particular day. This case study also highlights the interdependencies between meteorology and chemistry in the production of O_3; O_3 concentrations are often largest 50−100 km downwind of a NO_X emissions source.

DISCUSSION

In this work, we show the potential of TROPOMI NO_2 to provide new information to help air quality policy development. We develop top-down NO_X emissions estimates for two power plants and three megacities in North America for seasonal and sub-seasonal timeframes using TROPOMI. Using the operational TROPOMI NO_2 product that is enhanced by ECCC, we report a statistically insignificant low bias in our calculation of NO_X emissions from two U.S. power plants. For New York City, Chicago, and Toronto, we report NO_X emissions to be 18 ± 5, 19 ± 5 and 14 ± 5 Mg/h respectively. We find mean top-down NO_X emissions from New York City to be lower than the projected NEI estimates, although not in a statistically significant manner. For Chicago, we find better agreement with the NEI, and for Toronto, we find an underestimate in reported NO_X emissions. It is important to note that the bottom-up inventory estimates are annual average projections from earlier year inventories. For Chicago, we are also able to distinguish the weekday versus weekend effect of NO_X emissions within a single five-month period (45% larger on weekdays versus weekends in Chicago). Finally, in a last step, we discovered a day (July 7, 2018), in which a NO_X emissions rate could be derived for Chicago using a single TROPOMI overpass.

It should be noted that these metropolitan areas are near large water features and are subject to sea and lake breezes, which adds uncertainty to these analyses. Errors in the mean wind speed and variabilities in wind direction are the largest uncertainties that may systematically bias our estimates. Variabilities in the wind direction are partially accounted for in the effective photochemical lifetime.[4] As a next step, we suggest coupling the top-down approach with wind fields from NOAA's 3 km High-Resolution Rapid Refresh (HRRR) model.

While past studies using OMI needed 12+ months of data to develop top-down NO_X estimates, TROPOMI's considerably smaller pixels sizes and reduced instrument noise allows us to derive top-down NO_X emissions using less than 5 months of data, and sometimes even much less than that—in one case just a single day. This advancement is particularly exciting because TROPOMI can provide first estimates of seasonal NO_X emissions before more rigorous bottom-up emissions inventories are released. Furthermore, the capability to calculate top-down emissions rates over short timeframes allows us to develop estimates from transient sources such as wildfires and intermittent industrial activities, which are notoriously difficult to quantify in any other way. As TROPOMI continues to observe our atmosphere, we can expect to develop more estimates of NO_X emissions for cities and power plants worldwide that can be especially helpful for policymakers in assessing the effectiveness of regulations on NO_X emissions.

ASSOCIATED CONTENT

Supporting Information

The Supporting Information is available free of charge on the ACS Publications website at DOI: 10.1021/acs.est.9b04488.

Calculation of top-down NO_X emissions using the operational TROPOMI NO_2 retrieval algorithm and average May to Sept 2018 top-down NO_X emissions estimates from two isolated power plant complexes in the western U.S. using the operational TROPOMI tropospheric vertical column NO_2 product (PDF)

DOI: 10.1021/acs.est.9b04488
Environ. Sci. Technol. XXXX, XXX, XXX−XXX

AUTHOR INFORMATION

Corresponding Author

*E-mail: dgoldberg@anl.gov. Phone: (202)488-2417. Fax: (630) 252-8007.

ORCID

Daniel L. Goldberg: 0000-0003-0784-3986
David G. Streets: 0000-0002-0223-1350

Notes

The authors declare no competing financial interest.

ACKNOWLEDGMENTS

This manuscript was funded by the Department of Energy, Office of Fossil Energy. This manuscript was also partially using funding from the NASA Atmospheric Composition Modeling and Analysis Program (ACMAP). This manuscript was also developed under Assistance agreement no. RD835871 awarded by the U.S. Environmental Protection Agency to Yale University. It has not been formally reviewed by EPA. The views expressed in this document are solely those of the SEARCH Center and do not necessarily reflect those of the Agency. EPA does not endorse any products or commercial services mentioned in this manuscript. We would like to thank Junhua Zhang of Environment Canada for providing the emissions for the Toronto metropolitan area and three anonymous reviewers for their constructive comments. TROPOMI NO_2 data can be freely downloaded from the ESA Copernicus Open Access Hub or the NASA EarthData Portal (http://doi.org/10.5270/S5P-s4ljg54). NO_X bottom-up emissions data can be found here: https://www.epa.gov/air-emissions-inventories/air-pollutant-emissions-trends-data. Annual CEMS data from power plants can be downloaded here: https://ampd.epa.gov/ampd/. The submitted manuscript has been created by UChicago Argonne, LLC, Operator of Argonne National Laboratory ("Argonne"). Argonne, a US Department of Energy Office of Science laboratory, is operated under contract no. DE-AC02-06CH11357.

REFERENCES

(1) Jacob, D. J. *Introduction to Atmospheric Chemistry*; Princeton University Press, 1999.

(2) Beirle, S.; Boersma, K. F.; Platt, U.; Lawrence, M. G.; Wagner, T. Megacity Emissions and Lifetimes of Nitrogen Oxides Probed from Space. *Science* **2011**, *333*, 1737−1739.

(3) Valin, L. C.; Russell, A. R.; Cohen, R. C. Variations of OH Radical in an Urban Plume Inferred from NO_2 Column Measurements. *Geophys. Res. Lett.* **2013**, *40*, 1856−1860.

(4) de Foy, B.; Wilkins, J. L.; Lu, Z.; Streets, D. G.; Duncan, B. N. Model Evaluation of Methods for Estimating Surface Emissions and Chemical Lifetimes from Satellite Data. *Atmos. Environ.* **2014**, *98*, 66−77.

(5) Burrows, J. P.; Weber, M.; Buchwitz, M.; Rozanov, V.; Ladstätter-Weißenmayer, A.; Richter, A.; DeBeek, R.; Hoogen, R.; Bramstedt, K.; Eichmann, K.-U.; et al. The Global Ozone Monitoring Experiment (GOME): Mission Concept and First Scientific Results. *J. Atmos. Sci.* **1999**, *56*, 151−175.

(6) Valin, L. C.; Russell, A. R.; Hudman, R. C.; Cohen, R. C. Effects of Model Resolution on the Interpretation of Satellite NO2 Observations. *Atmos. Chem. Phys.* **2011**, *11*, 11647−11655.

(7) Vandaele, A. C.; Hermans, C.; Simon, P. C.; Carleer, M.; Colin, R.; Fally, S.; Mérienne, M. F.; Jenouvrier, A.; Coquart, B. Measurements of the NO2 Absorption Cross-Section from 42 000 Cm−1 to 10 000 Cm−1 (238−1000 Nm) at 220 K and 294 K. *J. Quant. Spectrosc. Radiat. Transfer* **1998**, *59*, 171−184.

(8) Veefkind, J. P.; Aben, I.; McMullan, K.; Förster, H.; de Vries, J.; Otter, G.; Claas, J.; Eskes, H. J.; de Haan, J. F.; Kleipool, M.; et al. TROPOMI on the ESA Sentinel-5 Precursor: A GMES Mission for Global Observations of the Atmospheric Composition for Climate, Air Quality and Ozone Layer Applications. *Remote Sens. Environ.* **2012**, *120*, 70−83.

(9) Van Geffen, J. H. G. M.; Eskes, H. J.; Boersma, K. F.; Maasakkers, J. D.; Veefkind, J. P. *TROPOMI ATBD of the Total and Tropospheric NO_2 Data Products*, 2019.

(10) Martin, R. V.; Chance, K.; Jacob, D. J.; Kurosu, T. P.; Spurr, R. J. D.; Bucsela, E.; Gleason, J. F.; Palmer, P. I.; Bey, I.; Fiore, A. M.; et al. An Improved Retrieval of Tropospheric Nitrogen Dioxide from GOME. *J. Geophys. Res.: Atmos.* **2002**, *107* (). https://doi.org/10.1029/2001JD001027. DOI: 10.1029/2001jd001027

(11) Richter, A.; Burrows, J. P. Tropospheric NO_2 from GOME measurements. *Adv. Space Res.* **2002**, *29*, 1673.

(12) Bovensmann, H.; Burrows, J. P.; Buchwitz, M.; Frerick, J.; Noël, S.; Rozanov, V. V.; Chance, K. V.; Goede, A. P. H. SCIAMACHY: Mission Objectives and Measurement Modes. *J. Atmos. Sci.* **1999**, *56*, 127−150.

(13) Heue, K.-P.; Richter, A.; Bruns, M.; Burrows, J. P.; Friedeburg, C. V.; Platt, U.; Pundt, I.; Wang, P.; Wagner, T. Validation of SCIAMACHY Tropospheric NO2 Columns with AMAXDOAS Measurements. *Atmos. Chem. Phys.* **2005**, *5*, 1039−1051.

(14) Richter, A.; Begoin, M.; Hilboll, A.; Burrows, J. P. An Improved NO_2 Retrieval for the GOME-2 Satellite Instrument. *Atmos. Meas. Tech.* **2011**, *4*, 1147−1159.

(15) Munro, R.; Lang, R.; Klaes, D.; Poli, G.; Retscher, C.; Lindstrot, R.; Huckle, R.; Lacan, A.; Grzegorski, M.; Holdak, A.; et al. The GOME-2 Instrument on the Metop Series of Satellites: Instrument Design, Calibration, and Level 1 Data Processing − an Overview. *Atmos. Meas. Tech.* **2016**, *9*, 1279−1301.

(16) Levelt, P. F.; van den Oord, G. H. J.; Dobber, M. R.; Malkki, A.; Huib Visser, A.; Johan de Vries, H.; Stammes, P.; Lundell, J. O. V.; Saari, H.; Saari, H. The Ozone Monitoring Instrument. *IEEE Trans. Geosci. Remote Sens.* **2006**, *44*, 1093−1101.

(17) Levelt, P. F.; Joiner, J.; Tamminen, J.; Veefkind, J. P.; Bhartia, P. K.; Stein Zweers, D. C.; Duncan, B. N.; Streets, D. G.; Eskes, H.; van der A, R.; et al. The Ozone Monitoring Instrument: Overview of 14 Years in Space. *Atmos. Chem. Phys.* **2018**, *18*, 5699−5745.

(18) Krotkov, N. A.; Lamsal, L. N.; Celarier, E. A.; Swartz, W. H.; Marchenko, S. V.; Bucsela, E. J.; Chan, K. L.; Wenig, M.; Zara, M. The Version 3 OMI NO2standard Product. *Atmos. Meas. Tech.* **2017**, *10*, 3133−3149.

(19) Boersma, K. F.; Eskes, H. J.; Richter, A.; De Smedt, I.; Lorente, A.; Beirle, S.; Van Geffen, J. H. G. M.; Zara, M.; Peters, E.; Van Roozendael, M.; et al. Improving Algorithms and Uncertainty Estimates for Satellite NO2 Retrievals: Results from the Quality Assurance for the Essential Climate Variables (QA4ECV) Project. *Atmos. Meas. Tech.* **2018**, *11*, 6651−6678.

(20) Streets, D. G.; Canty, T.; Carmichael, G. R.; De Foy, B.; Dickerson, R. R.; Duncan, B. N.; Edwards, D. P.; Haynes, J. A.; Henze, D. K.; Houyoux, M. R.; et al. Emissions Estimation from Satellite Retrievals: A Review of Current Capability. *Atmos. Environ.* **2013**, *77*, 1011−1042.

(21) Liu, F.; Beirle, S.; Zhang, Q.; Van Der A, R. J.; Zheng, B.; Tong, D.; He, K. NOx Emission Trends over Chinese Cities Estimated from OMI Observations during 2005 to 2015. *Atmos. Chem. Phys.* **2017**, *17*, 9261−9275.

(22) Verstraeten, W. W.; Boersma, K. F.; Douros, J.; Williams, J. E.; Eskes, H.; Liu, F.; Beirle, S.; Delcloo, A. Top-down NOx Emissions of European Cities Based on the Downwind Plume of Modelled and Space-Borne Tropospheric NO2 Columns. *Sensors* **2018**, *18*, 2893.

(23) de Foy, B.; Lu, Z.; Streets, D. G.; Lamsal, L. N.; Duncan, B. N. Estimates of Power Plant NOx Emissions and Lifetimes from OMI NO2 Satellite Retrievals. *Atmos. Environ.* **2015**, *116*, 1−11.

(24) Lu, Z.; Streets, D. G.; de Foy, B.; Lamsal, L. N.; Duncan, B. N.; Xing, J. Emissions of Nitrogen Oxides from US Urban Areas:

DOI: 10.1021/acs.est.9b04488
Environ. Sci. Technol. XXXX, XXX, XXX−XXX

Estimation from Ozone Monitoring Instrument Retrievals for 2005-2014. *Atmos. Chem. Phys.* **2015**, *15*, 10367−10383.
(25) McLinden, C. A.; Fioletov, V. E.; Boersma, K. F.; Krotkov, N.; Sioris, C. E.; Veefkind, J. P.; Yang, K. Air Quality over the Canadian Oil Sands: A First Assessment Using Satellite Observations. *Geophys. Res. Lett.* **2012**, *39*, .
(26) Liu, F.; Beirle, S.; Zhang, Q.; Dörner, S.; He, K.; Wagner, T. NOx Lifetimes and Emissions of Cities and Power Plants in Polluted Background Estimated by Satellite Observations. *Atmos. Chem. Phys.* **2016**, *16*, 5283−5298.
(27) Goldberg, D. L.; Saide, P. E.; Lamsal, L. N.; de Foy, B.; Lu, Z.; Woo, J.-H.; Kim, Y.; Kim, J.; Gao, M.; Carmichael, G.; et al. A Top-down Assessment Using OMI NO2 Suggests an Underestimate in the NOx Emissions Inventory in Seoul, South Korea, during KORUS-AQ. *Atmos. Chem. Phys.* **2019**, *19*, 1801−1818.
(28) Griffin, D.; Zhao, X.; McLinden, C. A.; Boersma, F.; Bourassa, A.; Dammers, E.; Degenstein, D.; Eskes, H.; Fehr, L.; Fioletov, V.; et al. High-Resolution Mapping of Nitrogen Dioxide With TROPOMI: First Results and Validation Over the Canadian Oil Sands. *Geophys. Res. Lett.* **2019**, *46*, 1049−1060.
(29) Kleipool, Q. L.; Dobber, M. R.; de Haan, J. F.; Levelt, P. F. Earth Surface Reflectance Climatology from 3 Years of OMI Data. *J. Geophys. Res.* **2008**, *113*, DOI: 10.1029/2008JD010290.
(30) McLinden, C. A.; Fioletov, V.; Boersma, K. F.; Kharol, S. K.; Krotkov, N.; Lamsal, L.; Makar, P. A.; Martin, R. V.; Veefkind, J. P.; Yang, K. Improved Satellite Retrievals of NO_2 and SO_2 over the Canadian Oil Sands and Comparisons with Surface Measurements. *Atmos. Chem. Phys.* **2014**, *14*, 3637−3656.
(31) Dee, D. P.; Uppala, S. M.; Simmons, A. J.; Berrisford, P.; Poli, P.; Kobayashi, S.; Andrae, U.; Balmaseda, M. A.; Balsamo, G.; Bauer, P.; et al. The ERA-Interim Reanalysis: Configuration and Performance of the Data Assimilation System. *Q. J. R. Meteorol. Soc.* **2011**, *137*, 553−597.
(32) National Centers for Environmental Information. Climate at a Glance https://www.ncdc.noaa.gov/cag/city/time-series/USW00094728/pcp/5/9/1980-2019?base_prd=true&firstbaseyear=1901&lastbaseyear=2000 (accessed July 24, 2019).
(33) Anderson, D. C.; Loughner, C. P.; Diskin, G.; Weinheimer, A.; Canty, T. P.; Salawitch, R. J.; Worden, H. M.; Fried, A.; Mikoviny, T.; Wisthaler, A.; et al. Measured and Modeled CO and NOy in DISCOVER-AQ: An Evaluation of Emissions and Chemistry over the Eastern US. *Atmos. Environ.* **2014**, *96*, 78−87.
(34) Travis, K. R.; Jacob, D. J.; Fisher, J. A.; Kim, P. S.; Marais, E. A.; Zhu, L.; Yu, K.; Miller, C. C.; Yantosca, R. M.; Sulprizio, M. P.; et al. Why Do Models Overestimate Surface Ozone in the Southeast United States? *Atmos. Chem. Phys.* **2016**, *16*, 13561−13577.
(35) Zhang, J.; Moran, M. D.; Zheng, Q.; Makar, P. A.; Baratzadeh, P.; Marson, G.; Liu, P.; Li, S.-M. Emissions Preparation and Analysis for Multiscale Air Quality Modeling over the Athabasca Oil Sands Region of Alberta, Canada. *Atmos. Chem. Phys.* **2018**, *18*, 10459−10481.
(36) Geddes, J. A.; Murphy, J. G.; O'Brien, J. M.; Celarier, E. A. Biases in Long-Term NO2 Averages Inferred from Satellite Observations Due to Cloud Selection Criteria. *Remote Sens. Environ.* **2012**, *124*, 210−216.
(37) Russell, A. R.; Valin, L. C.; Cohen, R. C. Trends in OMI NO2 Observations over the United States: Effects of Emission Control Technology and the Economic Recession. *Atmos. Chem. Phys.* **2012**, *12*, 12197−12209.
(38) de Foy, B.; Lu, Z.; Streets, D. G. Impacts of Control Strategies, the Great Recession and Weekday Variations on NO2 Columns above North American Cities. *Atmos. Environ.* **2016**, *138*, 74−86.

DOI: 10.1021/acs.est.9b04488
Environ. Sci. Technol. XXXX, XXX, XXX−XXX